Desalination and Water Treatment
www.deswater.com

doi: 10.5004/dwt.2019.24654

168 (2019) 348–356
November

Transformation of leaf waste into 3D graphene for water treatment

Xuechun Wang[a,b], Baosen Liu[c], Baoyou Shi[b,d], Laizhou Song[a,*], Yuan Zhuang[b,*]

[a]*College of Environmental and Chemical Engineering, Yanshan University, Qinhuangdao, China, emails: songlz@ysu.edu.cn (L.Z. Song), wxc19950620@163.com (X.C. Wang)*
[b]*Key Laboratory of Drinking Water Science and Technology, Research Center for Eco-Environmental Sciences, Chinese Academy of Sciences, Beijing, 100085, China, emails: yuanzhuang@rcees.ac.cn (Y. Zhuang), byshi@rcees.ac.cn (B.Y. Shi)*
[c]*State Key Laboratory of Pollution Control and Resource Reuse, School of Environmental Science and Engineering, Tongji University, 1239 Siping Road, Shanghai 200092, China, email: baosen163@163.com*
[d]*University of Chinese Academy of Sciences, Beijing 100049, China*

Received 19 March 2019; Accepted 29 June 2019

ABSTRACT

Transformation of waste into adsorbent achieves treating waste by waste. Here, 3D graphene with a large specific area was derived from waste leaf and employed for tetracycline removal from the aqueous solution. The influence of pH value on this antibiotic was evaluated, and then the adsorption behavior was studied by the analyses of two kinetics models (pseudo-first-order and pseudo-second-order equations) and two isotherm models (Langmuir and Freundlich). The Langmuir and the pseudo-second-order were best fitted for tetracycline uptake of the waste leaf graphene (WLG). The maximum adsorption capacity of WLG calculated from the Langmuir model was 909.09 mg/g. For the treatment of groundwater, WLG has an effective removal of organic pollutants and heavy metals, which indicates the fascinating potential application in water treatment. The facile preparation routine of graphene with low-cost and nontoxic characters is also resulting in macroscopic shape and excellent adsorption performance of the obtained 3D graphene. The study would offer a new version for the fabrication of graphene with the purpose of waste reclamation, and the obtained functional 3D graphene can be tremendously used in environmental pollution treatment and other areas.

Keywords: Waste; 3D graphene; Adsorption; Antibiotic removal

1. Introduction

With the development of global medical technology and the wide application of antibiotics, the harmful productions such as spent wastes and discharged wastewater have been increased rapidly. Among them, pharmaceutical effluent, especially the antibiotic wastewater, which brought serious harm to human body and ecological environment. Antibiotics belong to a group of antimicrobial compounds commonly used to treat diseases caused by microorganisms. The antibiotic has been widely used around the world because of its low cost and high efficiency in various infectious disease treatments [1]. Tetracycline (TC), the second most widely used antibiotics worldwide, has been used extensively in the treatment of human and animal diseases; while, over the past few decades, insufficient efforts have been focused on the disposal of antibiotic-containing effluents. According to recent research and literature reports, TC residues in the environment have caused a variety of potential adverse effects such as chronic toxicity [2] and dissemination into antibiotic-resistant genes [3]. Generally, it is very difficult to remove TC from water because of its variable state, low biodegradability and complex molecular structure [4]. Although the study of antibiotics has never

* Corresponding authors.

stopped, acute and chronic effects of antibiotics-containing wastewater on the ecology and the potential threat have not yet been fully understood [5]. Thus, it is of great importance to develop robust, efficient and cost-effective technologies for the removal of TC from wastewater.

Among various technologies employed to remove TCs from wastewater, including adsorption, biodegradation, photodegradation, and oxidative degradation, adsorption is a widely used effective technology, due to the advantages of easy operation, low-cost, high efficiency and no residual risk of highly toxic byproduct [6]. Carbon materials such as active carbon and graphene present unique advantages in adsorption due to their low cost, high adsorption capacity and easy disposal [7,8]. In general, it has been found that increasing the oxygen content of samples has detrimental effects on adsorption [9]. A dispersive interaction (mainly Van der Waals interaction) has been reported between the free electron of TC and the delocalized electron in carbon basal planes [10], which is valuable for the capture of organic pollutants.

Adsorbent prepared from waste has attracted considerable attention on account of the reuse in wastes [11–13]. Increasing number of researches have used different biomass wastes to prepare biochar as adsorption materials in the field of pollution control, demonstrating the advantages of a wide range of sources, low cost, and renewable feature. Moreover, the obtained biochar has a loose, porous structure and contains carboxyl, hydroxyl and other reactive groups, which can not only reduce the environmental burden but also achieve the effect of "treating waste by waste" [14]. However, most of the endeavors concentrate on the preparation of biochar with biomass wastes, till now, few studies focus on the transformation of waste into graphene.

In the past several years, a free-standing two-dimensional monolayer graphene with excellent mechanical, electrical, and thermal properties has caught global attention and has been adopted for various applications [15]. Also, with great specific surface area, graphene has been considered as an excellent adsorbent [16]. With its delocalized π bonds, graphene can potentially adsorb organic contaminants, especially these with molecules containing π-electrons that can interact with a polarized graphene surface via π-π electron coupling or Van der Waals interactions [17,18]. Thus, the graphene-based material as an adsorbent can effectively remove organic substances and heavy metal ions present in the wastewater. However, they are easily agglomerated during use, resulting in a sharp decrease in specific surface area and thus lowering the adsorption performance. Moreover, another defect is that it is unfeasible to separate spent graphene-type materials from wastewater after the adsorption is completed. For application as an adsorbent, compared with conventional carbon adsorbents, the three-dimensional (3D) graphene is easily separable [19]. The defects of difficult dispersion for graphene sheets and their poor interfacial interactions with matrix retard its application. Exfoliation of graphene could produce stable suspensions of quasi two-dimensional carbon sheets, making this a critical aspect for the large-scale synthesis of graphene sheets [20]. Much research has been focused on developing routes for obtaining large sheets of monolayer graphene. This has been recently achieved by chemical vapour deposition (CVD), using polymer as carbon source could obtain graphene with controllable thickness [21]. It is an effective way for biomass reuse through the easy preparation of graphene.

In this study, 3D graphene is prepared using waste leaf to remove antibiotic from water. The structure and morphology of fabricated waste leaf graphene (WLG) were characterized using a scanning electron microscopy (SEM) and transmission electron microscopy (TEM) measurement, the specific surface area of this sample was characterized by the Brunauer–Emmett–Teller (BET) method. Its electrochemical feature was assessed by an electrochemical workstation. The adsorption performance of WLG toward TC was evaluated by a series of batch experiments, then data of adsorption kinetics and isotherm adsorption tests were analyzed. Lastly, the potential application of WLG in groundwater treatment was attempted. The resulting graphene possesses desirable excellent adsorption properties for TC. We believe that the easy preparation of graphene proposed by this research would promote the reuse of biomass wastes in the field of water treatment.

2. Materials and methods

2.1. Materials

All chemical reagents used in this study were all analytical grade. Tetracycline hydrochloride (purity ≥ 95%) was purchased from Macklin Biochemical Co. Ltd. (Shanghai, China). Other chemicals were purchased from Sinopharm Chemical Reagent Co. Ltd. (Shanghai, China) and used in the experiments without any further purification. All solutions were prepared using deionized water.

2.2. Preparation of adsorbent

We collected the leaf waste from ground. The collected waste leaves were washed with deionized water for three times. Then they were dried in an oven at a temperature of 70°C for 2 h. After that, the treated waste ginkgo leaves were carbonized in the presence of nickel catalyst in 800°C under nitrogen atmosphere with constant flow of 45 mL/min.

2.3. Characterization

The structure and morphology of waste leaf graphene (WLG) were characterized using a SEM. TEM measurement was performed on a GZF2.0 (FEI Electron Optics, USA) instrument at an accelerating voltage of 200 kV. The specific surface area was characterized by the Brunauer–Emmett–Teller (BET) method. The relative pressure (P/P_0) ranged between 0 and 1, and the pore size distribution plots were derived from the adsorption branch of the isotherms based on the Barrett–Joyner–Halenda (BJH) model. Electrochemical measurements were performed at 298 K under atmospheric pressure, using an electrochemical workstation (CHI 660C, Chenhua Co. Ltd., Shanghai, China). A three-stand electrode cell was employed with WLG conductive slide as the working electrode, Ag/AgCl as the reference electrode, and Pt wire as the auxiliary electrode. The working electrode was prepared by ultrasonically mixing the WLG with the Nafion solution and applying it to a conductive slide. Surface functional groups on WLG were identified using a Fourier

transform infrared spectrometer (FTIR, iS10, Thermo, USA) equipped with an attenuated total reflectance accessory with smart iTX optical base and AR diamond crystal plate. FTIR spectra from 32 scans were recorded in the wavenumber range 400–4,000 cm^{-1} with 2 cm^{-1} resolution [22].

2.4. Sorption experiments

2.4.1. Sorption kinetics

Batch experiments were conducted to evaluate the performance of waste leaf 3D graphene (WLG) for the adsorption of TC. After adsorption, the adsorbent was separated from the solution using a 0.45 μm membrane then the concentrations of the TC were determined using a UV–Vis spectrophotometer (Mapada, UV-6100) at a wavelength of 356 nm. Batch adsorption studies were carried out using the following experimental procedure: 20 mg WLG was added to a 20 mL of initial concentration 100 mg L^{-1} TC solution, then shaken at 150 rpm with a certain time at 298 K. Kinetic experiments were conducted under designated reaction times (0.08, 0.16, 0.25, 0.33, 0.5, 1, 2, 3, 5, 7, 9, 12, 20, 24 h). Isotherm experiments were carried out at a series of TC initial concentrations (1, 5, 10, 50, 100, 200, 400, 600, 800 and 1,000 mg L^{-1}), while keeping the WLG addition as 1 mg/L, reaction time as 12 h, and the temperature at 298 K.

The effect of adsorbent dosage was studied by varying the WLG addition from 0.1 to 0.5 g/L. The adsorption capacity was calculated using the following equation:

$$q_t = \frac{(C_0 - C_t) \times V}{m} \tag{1}$$

where C_0 and C_t (mg L^{-1}) are initial and equilibrium concentrations of TC, respectively, q_t (mg g^{-1}) is the adsorbed amount of adsorbate per unit mass of the adsorbent at time t, m (g) is the mass of adsorbent, and V (L) is the volume of working solution.

To identify the time for reaching adsorption equilibrium and in order to understand the characteristics of the adsorption process, the data are fitted with pseudo-first-order and pseudo-second-order models. These two models can be expressed as Eqs. (2) and (3), respectively.

$$\log(q_e - q_t) = \log q_e - k_1 t \tag{2}$$

$$\frac{t}{q_t} = \frac{1}{k_2 q_e^2} + \frac{t}{q_e} \tag{3}$$

where q_t and q_e (mg g^{-1}) are the amounts of TC adsorbed at time t and equilibrium state, respectively. k_1 (h^{-1}) and k_2 (g mg^{-1} h^{-1}) are the rate constants of pseudo-first-order and pseudo-second-order equations, respectively.

2.4.2. Adsorption isotherms

To understand the relationship between adsorbent and adsorbate, the obtained adsorption data were fitted by the Langmuir and Freundlich models, and they are depicted as follows:

Langmuir isotherm equation:

$$q_e = \frac{q_{\max} K_L C_e}{\left(1 + K_L \times C_e\right)} \tag{4}$$

The linear forms of Langmuir model is:

$$\frac{1}{q_e} = \frac{1}{q_{\max} \times K_L} \times \frac{1}{C_e} + \frac{1}{q_{\max}} \tag{5}$$

where q_e (mg g^{-1}) is the equilibrium adsorption capacity. $q_{\max}$ (mg g^{-1}) is the maximum adsorption capacity. K_L is the Langmuir adsorption equilibrium constant and C_e (mg L^{-1}) is the equilibrium solution concentration.

To evaluate the feasibility of adsorption, an equilibrium parameter R_L can be calculated using Eq. (6).

$$R_L = \frac{1}{1 + K_L C_0} \tag{6}$$

The value of R_L indicates the type of the isotherm: $R_L = 0$, adsorption is irreversible; $0 < R_L < 1$, adsorption is favorable; $R_L = 1$, adsorption is linear, $R_L > 1$, adsorption is unfavorable.

The Freundlich isotherm, based on adsorption in a heterogeneous surface, is expressed in linear from as Eq. (7).

$$\ln q_e = \ln K_F + \frac{1}{n} \ln C_e \tag{7}$$

where K_F ($mg^{(1-1/n)}$ $L^{1/n}$ g^{-1}) and n are Freundlich constants. Values of n in Freundlich model can give an indication of how favorable the adsorption process is. It has been reported that values of n in the range of 1–10 represent favorable under selected experimental conditions.

The Temkin isotherm contains a factor that explicitly takes into account of the adsorbent–adsorbate interactions. The linear form of the Temkin model is written as:

$$q_e = \frac{RT}{bT} \ln AT + \frac{RT}{bT} \ln C_e \tag{8}$$

where $B = RT/b_T$, b_T is the Temkin constant related to the heat of adsorption (J mol^{-1}), A_T is the Temkin isotherm equilibrium binding constant (L g^{-1}), R is the gas constant (8.3145 J mol^{-1} K^{-1}) and T is the absolute temperature at 303 K. From the plot of Q_e vs. $\ln C_e$, B and A_T can be calculated from the slope (B) and intercepts ($B \ln A_T$), respectively.

2.4.3. Effect of solution pH

The effect of pH on TC adsorption (10 mg L) onto WLG was examined at different pH values (pH 2–10), keeping the reaction time for 24 h. The pH of the TC solution was adjusted to a certain value using 1.0 M HCl and 1.0 M NaOH solution.

2.4.4. Groundwater adsorption experiment

20 mg WLG was added to a 20 mL solution of groundwater, then shaken at 150 rpm at 298 K. After the adsorption, the

adsorbent was separated from the solution using a 0.45 μm membrane then tested by an excitation–emission matrix (EEM) fluorescence spectrophotometer (F-4500, Hitachi, Japan). The metal ion concentration of the groundwater treated by WLG before and after adsorption was tested by the inductively coupled plasma (Thermo Fisher ICP-MS, Thermo Fisher Scientific Co. Ltd.).

3. Results and discussion

Formation process of waste leaf to WLG was illustrated by Fig. 1. Before and after CVD, the leaf turns from yellow into black and remains the original shape. As indicated by Fig. 1, the fabricated WLG has a 3D macroscopic structure, which would make the separation of adsorbent from water easily. Also, it can be seen from the insert SEM image that the leaf has a smooth surface, but the WLG has abundant non-uniform pores of 10 μm. The existence of abundant pores in the WLG is benefit for the enhancement in adsorption capacity.

Herein, TEM was used to characterize the morphology of the leaf carbon source and WLG. As shown by Fig. 2a, the leaf has a notable network structure. After CVD treatment (Fig. 2b), the WLG has a fiber-like surface accompanied by the presence of sheet-like center. It could suggest that the structure of the carbon source has great influence on the obtained graphene. Thus, it can be inferred that the porous leaf is beneficial to inhibit the agglomeration of graphene.

Fig. 3a shows the N_2 adsorption–desorption isotherms of WLG. The isotherm showed the presence of a hysteresis loop, which is a characteristic feature of the type IV isotherms. The adsorption isotherms indicated that the pores are mesoporous. The specific area of WLG is 205.69 m^2/g, which is larger than other antibiotic adsorbents such as graphene hydrogel (119.17 m^2/g) [23], graphene/soy protein composite (30.07 m^2/g) [24], magnetic graphene oxide/diethylenetriaminepentaacetic acid nanocomposite (176 m^2/g) [25], and 3D urchin-like iron oxides (139.99 m^2/g) [26]. As reported by Fig. 3b, the presence of disorder sp^2-hybridized carbon systems leads to interesting and intriguing phenomena in the

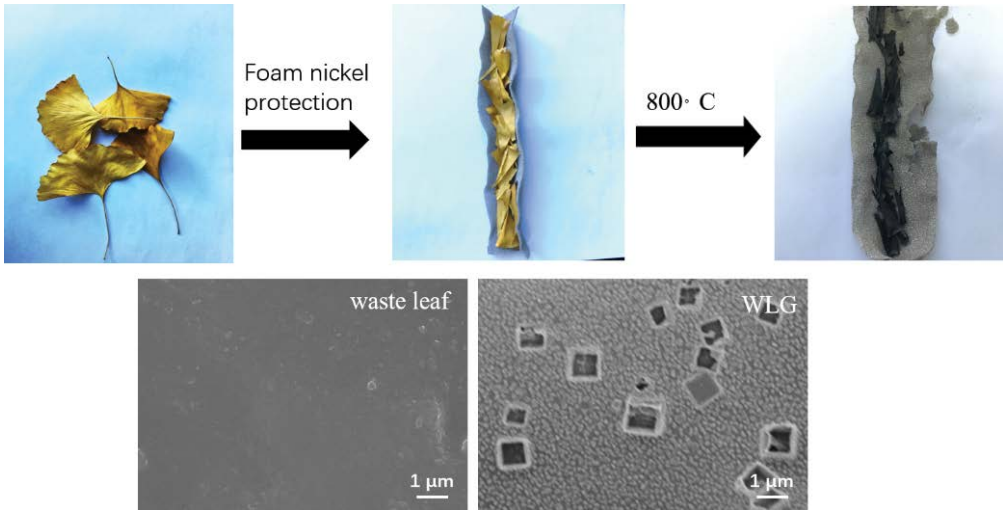

Fig. 1. Photograph and SEM of the waste leaf and the WLG.

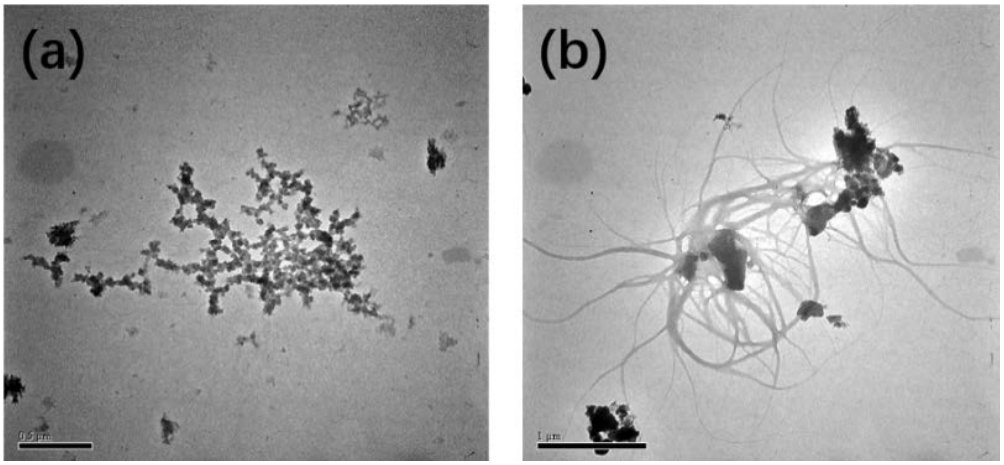

Fig. 2. TEM images of the waste leaf (a) and the WLG (b).

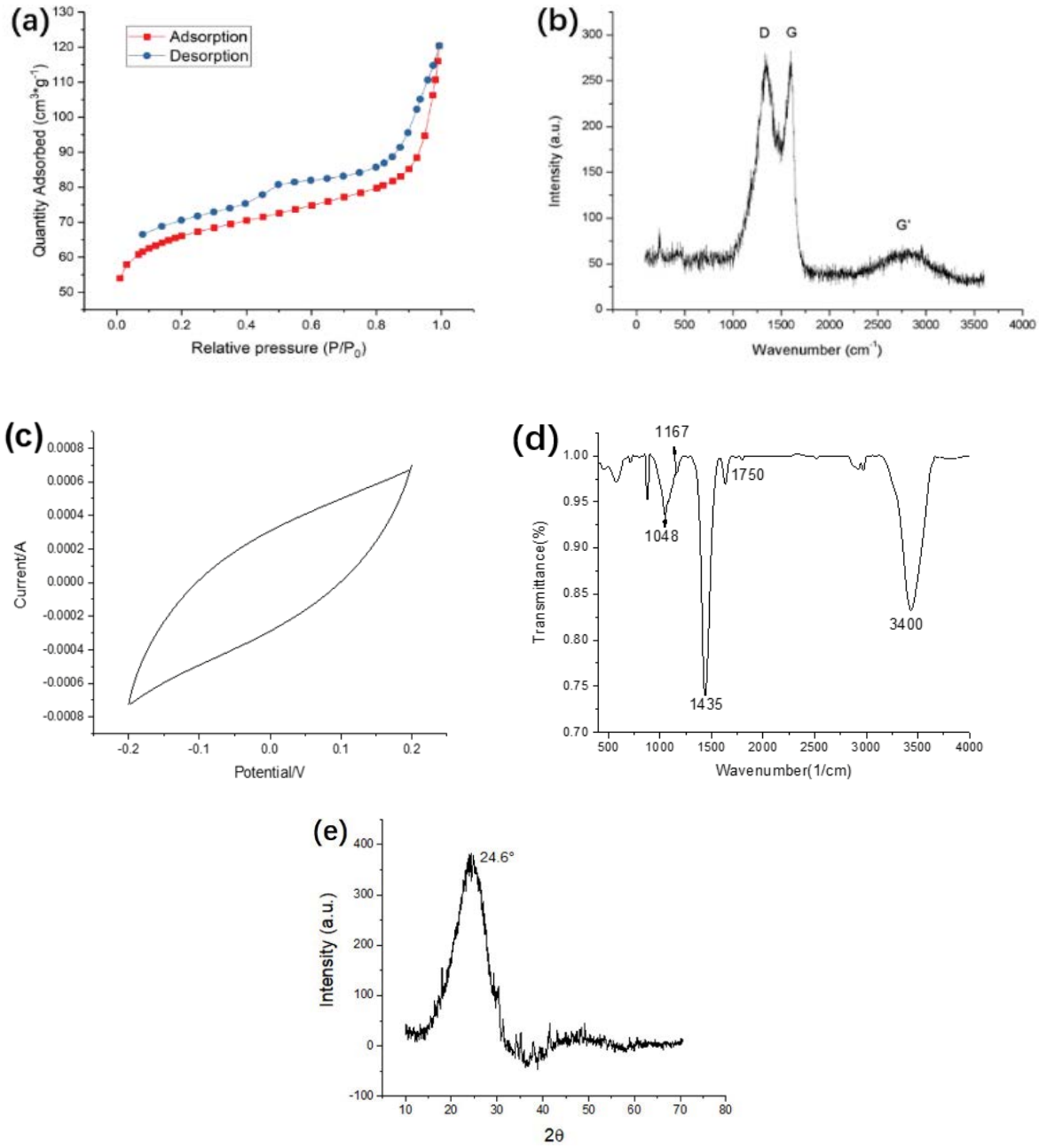

Fig. 3. (a) N_2 adsorption–desorption isotherms, (b) Raman spectra, (c) cyclic voltammetry curve of WLG, (d) Fourier transform infrared spectroscopy (FTIR) spectra of WLG, and (e) XRD of WLG.

resonance Raman spectra: the Raman spectra of the disordered graphene exhibit two new sharp features appearing at 1,345 and 1,626 cm^{-1}, thereby attesting the appearance of point defects. These two features have been called D and G bands, usually used to denote the disorder of lamellar structure. The existence of sharp D and G peaks further confirm the formation of graphene. The voltammetry curve of WLG shown in Fig. 3c, indicates the excellently electrical properties which is corresponded to the unique two-dimensional structure of graphene sheets [23,27]. The FTIR spectra were analyzed to identify the characteristic functional groups of the adsorbents. The 400–4,000 cm^{-1} infrared spectral regions of the WLG were shown in Fig. 3d. Several obvious peaks can be observed in the infrared spectra of WLG. As shown in Fig. 3d, the functional groups, including the stretching vibrations of –OH (3,400 cm^{-1}), $-SO_3H$ (1,750 cm^{-1}), the C–H groups in aromatic rings (1,435 cm^{-1}) and C–O in phenol (1,167 cm^{-1}), are clearly identified. The peak at 1,048 cm^{-1} are assigned to the C–O stretching [28–31]. XRD result is shown in Fig. 3e. The diffraction peaks are due to the graphene sheet space of 0.36 nm.

Influence of contact time on adsorption capacity is shown in Fig. 4a. It can be seen that the adsorption capacity increases sharply within 5 h, slowly increases thereafter,

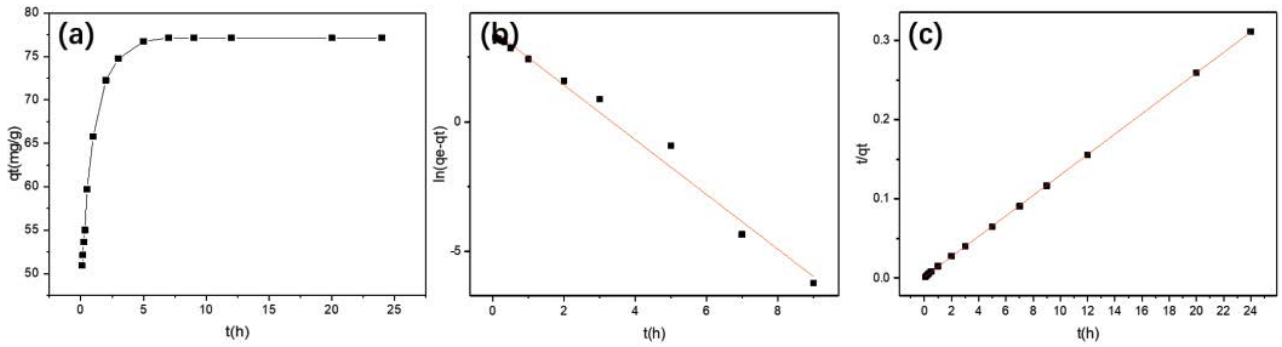

Fig. 4. Kinetic curves (a), kinetic analyses of pseudo-first order model (b), pseudo-second order model (c).

finally reaches equilibrium around 10 h. Based on these results, the kinetic data are fitted by two models. The linear plots are shown in Figs. 4b and c. All calculated model parameters are presented in Table 1. Among the two models, the pseudo-second-order plots show high correlation coefficients (R^2 = 0.999). As to the pseudo-first-order, the R^2 value is low and the calculated q_e value is much lower than that of the pseudo-second-order model; also, the q_e obtained by pseudo-second-order model is close to the determined value. It is implied that the pseudo-second-order rate model could fit better than the pseudo-first-order model to describe this adsorption process. This means that the adsorption rate might be determined by chemical adsorption process through electron transfer, exchange or sharing between adsorbent and adsorbate.

The isotherm data are fitted by Langmuir and Freundlich models, and the results are shown in Fig. 5. All calculated model parameters are reported in Table 2. For TC adsorption, the adsorption data are fitted well by the Langmuir isotherm. This result suggests that adsorption of TC occurs on homogenous surfaces and will form a covering monolayer at the surfaces of the WLG. The Langmuir constants R_L are all between one and zero, suggesting a favorable condition for adsorption. Based on this result, it can be inferred that maximum monolayer adsorption capacity of TC on WLG attains up to 909.09 mg g^{-1}, which is higher than most of the adsorbents such as activated carbon, biochar and graphene (shown in Table 3). The regression coefficients of the isotherm (>0.99) present a strong affinity between the tetracycline and WLG. In this study, both Freundlich and Langmuir model could exactly fit the sorption data of

Table 1
Kinetics parameters of TC adsorption onto WLG

Pseudo-first-order			Pseudo-second-order		
q_e/mg g^{-1}	k_1/min^{-1}	R^2	q_e/mg^{g-1}	k_2/min^{-1}	R^2
34.43	1.06	0.986	77.58	0.124	0.999

Table 2
Isotherm parameters of TC adsorption onto WLG

Langmuir			Freundlich			Temkin	
q_{max} /mg g^{-1}	K_L	R^2	K_F	n	R^2	K_T	R^2
909.09	0.001	0.999	102.497	1.090	0.998	0.1023	0.871

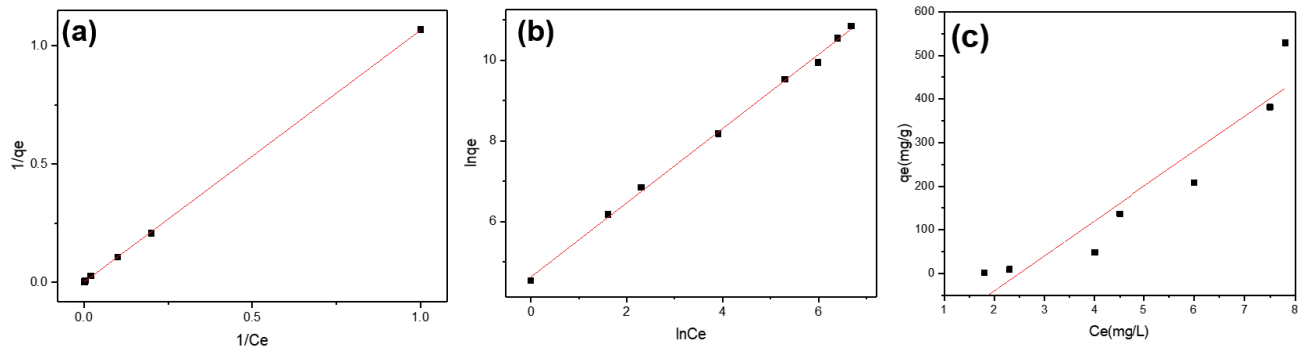

Fig. 5. Adsorption isotherms: (a) Langmuir model, (b) Freundlich model, (c) Temkin model.

Table 3
Comparison of different adsorbent for antibiotics

Adsorbent	q_m (mg/g)	Reference
Graphene-soy protein biocomposite	500	[23]
Graphite	400	[13]
Porous biochar	786.1	[34]
Core-shell activated carbon	95.4	[35]
Macroporous polystyrene resins	98.04	[36]
Modified bio-char	17.0	[37]
Activated carbon	475.48	[38]
WLG	909.09	This study

TC on WLG, which indicates the sorption of TC on WLG might be affected by a multiple mechanism. During TC adsorption onto WLG, both π–π and hydrogen bond interactions will play an important role in the capture of this antibiotic [32]. It is validated that electron donor–acceptor interaction is one of the driving forces for the sorption of organic chemicals with graphene [24], in this adsorption process, the –OH groups on the graphene surface can make the graphene acting as electron donors. Thus, significant enhanced sorption was expected by the formation of a π–π bond between TC and WLG. Moreover, functional groups such as –COOH and $–NH_2$ contained in tetracycline and WLG will be advantageous to form a hydrogen bond between them [18]. For the Temkin model, it is based on electrostatic interaction between opposite electrical charges for the chemical adsorption. The good coefficient with Temkin model indicating the heat of adsorption of all the four organic molecules in the layer would decrease linearly with coverage due to adsorbent–adsorbate interaction and the adsorption is driven by a uniform existence of binding energies [33].

The initial pH is one of the most significant variables influencing adsorption process. The effects of pH on TC adsorption capacity by WLG are studied at pH values from 2 to 10. Fig. 6 shows that the adsorption capacity decreases with increasing pH. The reason is that with the pH increases, deprotonation of carboxyl groups is enhanced. Thus, the electrostatic repulsion force between TC and WLG becomes remarkable and thus decreases the uptake of TC [39]. These results indicate that pH is a significant factor that influences adsorption process of TC by WLG, and an acid condition is suitable for the TC adsorption by WLG. Under pH 6, the tetracycline removal rate is 76.3%. Regeneration of the TC adsorption by WLG is shown in Fig. 6b, from which can be seen that the materials still has well adsorption capacity after five cycles.

The groundwater used for the experiment was taken from a province in north of China. The water quality indicators of groundwater are as follows: chemical oxygen demand and total organic carbon (TOC) are 15 and 2.126 mg/L, respectively; the pH of this solution is 8.2. The treatment efficiency of WLG on this groundwater is shown in Fig. 7. As shown in Figs. 7a and b, after treatment by WLG, the organic matter content is significantly reduced. The TOC value of groundwater has dropped significantly from 2.126 to 0.062 mg/L. Figs. 7c and d show the removal rates of U, Fe, As, Pb, Ga, Co and Ge metal ions under different WLG dosages. It can be seen that the adsorption capacities for all metal ions decrease gradually with the increase of adsorbent dosage in solution, which is attributed to the increase in weight of WLG. Herein, it should be mentioned that uranium is a toxic radioactivity element, and is usually found in the environment in the hexavalent form. From the viewpoint of full utilization of uranium resources and environmental protection, highly effective enrichment of uranium as well as its removal from aqueous solutions is of extreme importance. Carbon materials are chosen for this purpose because of their high radiation resistance [40]. After the adsorption by WLG, the concentration of uranium reduced from 14.69 to 0.023 μg, with a removal rate of 99.84%. The excellent removal for uranium and other ions by WLG is mainly dominated by the surface complexation and cation exchange of UO_2^{2+} with oxygen-containing functional groups of this adsorbent. It could be seen that, the WLG has an excellent efficiency in removal of heavy metals

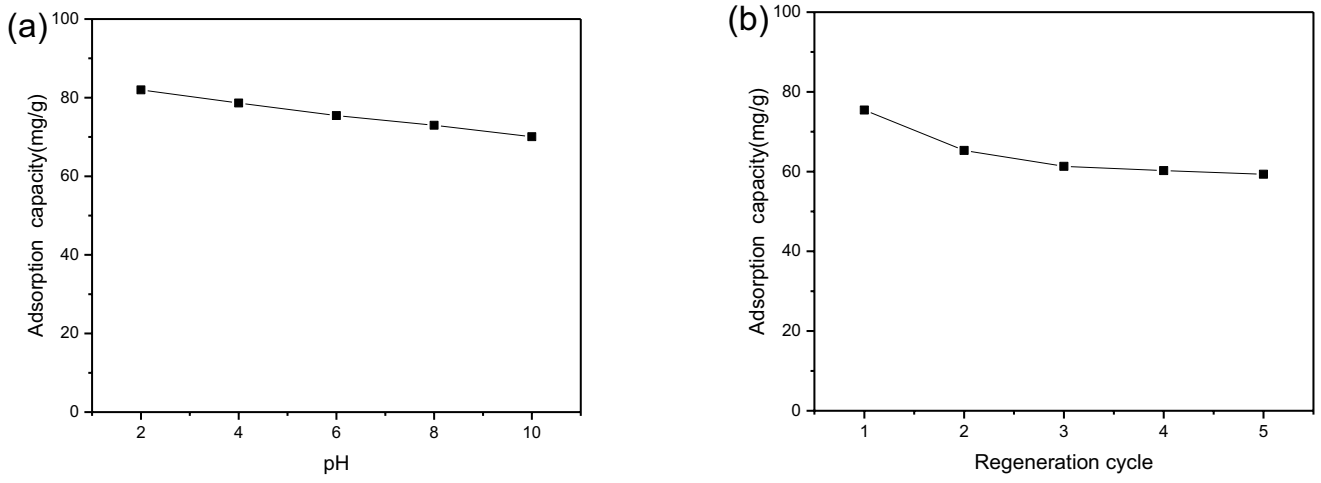

Fig. 6. (a) Influence of pH on adsorption, (b) regeneration.

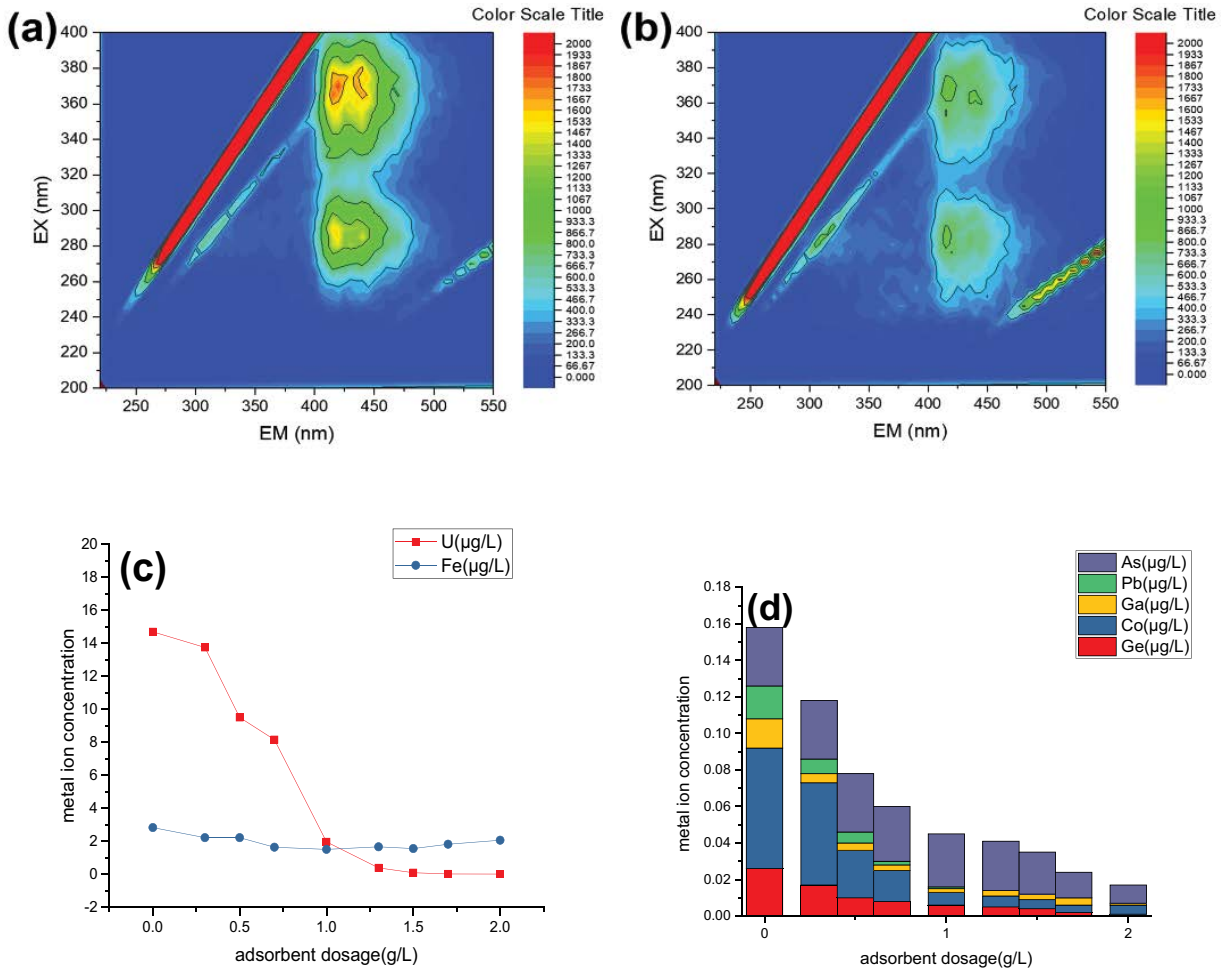

Fig. 7. Groundwater treatment. (a) EEM of raw water, (b) EEM of raw water after adsorption by WLG, (c) metal ion U and Fe removal rate under different adsorbent dosage, (d) metal ion As, Pb, Ga, Co, Ge removal rate under different adsorbent dosage.

and organic pollutants from groundwater. In view of the low-cost preparation by leaf waste, we believe that WLG has a potential application in the environmental cleanup.

4. Conclusions

This study aims at the reuse of waste leaf to prepare a 3D graphene adsorbent and to employ for the removal of TC antibiotic from the aqueous solution. The fabricated WLG material has a large specific area of 205.69 m^2/g, the maximum adsorption by WLG is 909.09 mg/g. In addition, WLG has a sufficient removal in organic pollutants and heavy metals (particular for the uptake of uranium) from groundwater. The preparation routine for graphene proposed in this study is low-cost and nontoxic, resulting in macroscopic shape and excellent adsorption performance of the 3D graphene. Beside the reclamation of leaf waste, this study can offer a new way for the treatment of wastewater.

Acknowledgments

This research was supported by the National Natural Science Foundation of China (51808538) and National Key Research and Development Program of China (2016 YFA0203204).

References

[1] Y. Kong, Y. Zhuang, J.W. Yu, Z.Y. Han, B.Y. Shi, Structural study on PVA assisted self-assembled 3D hierarchical iron (hydr) oxides, Crystengcomm, 20 (2018) 2093–2101.
[2] L. Wollenberger, B. Halling-Sorensen, K.O. Kusk, Acute and chronic toxicity of veterinary antibiotics to *Daphnia magna*, Chemosphere, 40 (2000) 723–730.
[3] A. Abdolali, W.S. Guo, H.H. Ngo, S.S. Chen, N.C. Nguyen, K.L. Tung, Typical lignocellulosic wastes and by-products for biosorption process in water and wastewater treatment: a critical review, Bioresour. Technol., 160 (2014) 57–66.
[4] T. Junker, R. Alexy, T. Knacker, K. Kummerer, Biodegradability of C-14-labeled antibiotics in a modified laboratory scale sewage treatment plant at environmentally relevant concentrations, Environ. Sci. Technol., 40 (2006) 318–324.
[5] A.J. Watkinson, E.J. Murby, S.D. Costanzo, Removal of antibiotics in conventional and advanced wastewater treatment: implications for environmental discharge and wastewater recycling, Water Res., 41 (2007) 4164–4176.
[6] Y. Zhuang, F. Yu, J. Ma, J.H. Chen, Facile synthesis of three-dimensional graphene-soy protein aerogel composites for tetracycline adsorption, Desal. Wat. Treat., 57 (2016) 9510–9519.

[7] I. Cabrita, B. Ruiz, A.S. Mestre, I.M. Fonseca, A.P. Carvalho, C.O. Ania, Removal of an analgesic using activated carbons prepared from urban and industrial residues, Chem. Eng. J., 163 (2010) 249–255.
[8] H.-H. Cho, B.A. Smith, J.D. Wnuk, D.H. Fairbrother, W.P. Ball, Influence of surface oxides on the adsorption of naphthalene onto multiwalled carbon nanotubes, Environ. Sci. Technol., 42 (2008) 2899–2905.
[9] S.A. Carabineiro, T. Thavorn-Amornsri, M.F. Pereira, J.L. Figueiredo, Adsorption of ciprofloxacin on surface-modified carbon materials, Water Res., 45 (2011) 4583–4591.
[10] S.A.C. Carabineiro, T. Thavorn-amornsri, M.F.R. Pereira, P. Serp, J.L. Figueiredo, Comparison between activated carbon, carbon xerogel and carbon nanotubes for the adsorption of the antibiotic ciprofloxacin, Catal. Today, 186 (2012) 29–34.
[11] Y. Zhuang, X.Q. Wu, Z.J. Cao, X.X. Zhao, M.H. Zhou, P. Gao, Preparation and characterization of sponge film made from feathers, Mater. Sci. Eng. C, 33 (2013) 4732–4738.
[12] C. Chen, T. Ma, Y. Shang, B. Gao, B. Jin, H. Dan, Q. Li, Q. Yue, Y. Li, Y. Wang, X. Xu, In-situ pyrolysis of *Enteromorpha* as carbocatalyst for catalytic removal of organic contaminants: considering the intrinsic N/Fe in *Enteromorpha* and non-radical reaction, Appl. Catal. B: Environ., 250 (2019) 382–395.
[13] Y. Zhuang, X.X. Zhao, M.H. Zhou, Cr(VI) adsorption on a thermoplastic feather keratin film, Desal. Wat. Treat., 52 (2014) 2786–2791.
[14] S. Sahota, V.K. Vijay, P.M.V. Subbarao, R. Chandra, P. Ghosh, G. Shah, R. Kapoor, V. Vijay, V. Koutu, I.S. Thakur, Characterization of leaf waste based biochar for cost effective hydrogen sulphide removal from biogas, Bioresour. Technol., 250 (2018) 635–641.
[15] L. Ji, W. Chen, L. Duan, D. Zhu, Mechanisms for strong adsorption of tetracycline to carbon nanotubes: a comparative study using activated carbon and graphite as adsorbents, Environ. Sci. Technol., 43 (2009) 2322–2327.
[16] F. Yu, Y. Sun, M. Yang, J. Ma, Adsorption mechanism and effect of moisture contents on ciprofloxacin removal by three-dimensional porous graphene hydrogel, J. Hazard. Mater., 374 (2019) 195–202.
[17] Y. Lin, S. Xu, J. Li, Fast and highly efficient tetracyclines removal from environmental waters by graphene oxide functionalized magnetic particles, Chem. Eng. J., 225 (2013) 679–685.
[18] H. Chen, B. Gao, H. Li, Functionalization, pH, and ionic strength influenced sorption of sulfamethoxazole on graphene, J. Environ. Chem. Eng., 2 (2014) 310–315.
[19] Y. Zhuang, F. Yu, H. Chen, J. Zheng, J. Ma, J.H. Chen, Alginate/graphene double-network nanocomposite hydrogel beads with low-swelling, enhanced mechanical properties, and enhanced adsorption capacity, J. Mater. Chem. A, 4 (2016) 10885–10892.
[20] Y. Zhuang, Y. Kong, K. Han, H.T. Hao, B.Y. Shi, A physically cross-linked self-healable double-network polymer hydrogel as a framework for nanomaterial, New J. Chem., 41 (2017) 15127–15135.
[21] Z.Z. Sun, Z. Yan, J. Yao, E. Beitler, Y. Zhu, J.M. Tour, Growth of graphene from solid carbon sources, Nature, 468 (2010) 549–552.
[22] Y. Han, A.A. Boateng, P.X. Qi, I.M. Lima, J. Chang, Heavy metal and phenol adsorptive properties of biochars from pyrolyzed switchgrass and woody biomass in correlation with surface properties, J. Environ. Manage., 118 (2013) 196–204.
[23] Y. Zhuang, F. Yu, J. Ma, J.H. Chen, Graphene as a template and structural scaffold for the synthesis of a 3D porous bio-adsorbent to remove antibiotics from water, RSC Adv., 5 (2015) 27964–27969.
[24] Y. Zhuang, F. Yu, J. Ma, J.H. Chen, Adsorption of ciprofloxacin onto graphene-soy protein biocomposites, New J. Chem., 39 (2015) 3333–3336.
[25] M.F. Li, Y.G. Liu, S.B. Liu, G.M. Zeng, X.J. Hu, X.F. Tan, L.H. Jiang, N. Liu, J. Wen, X.H. Liu, Performance of magnetic graphene oxide/diethylenetriaminepentaacetic acid nanocomposite for the tetracycline and ciprofloxacin adsorption in single and binary systems, J. Colloid Interface Sci., 521 (2018) 150–159.
[26] Y. Zhuang, Y. Kong, Q.Z. Liu, B.Y. Shi, Alcohol-assisted self-assembled 3D hierarchical iron (hydr)oxide nanostructures for water treatment, Crystengcomm, 19 (2017) 5926–5933.
[27] P. Duan, T. Ma, Y. Yue, Y. Li, X. Zhang, Y. Shang, B. Gao, Q. Zhang, Q. Yue, X. Xu, Fe/Mn nanoparticles encapsulated in nitrogen-doped carbon nanotubes as a peroxymonosulfate activator for acetamiprid degradation, Environ. Sci.: Nano, 6 (2019) 1799–1811.
[28] E. Malkoc, Y. Nuhoglu, Removal of Ni(II) ions from aqueous solutions using waste of tea factory: adsorption on a fixed-bed column, J. Hazard. Mater., 135 (2006) 328–336.
[29] C. Dong, J. Lu, B. Qiu, B. Shen, M. Xing, J. Zhang, Developing stretchable and graphene-oxide-based hydrogel for the removal of organic pollutants and metal ions, Appl. Catal. B: Environ., 222 (2018) 146–156.
[30] Y. Sun, H. Li, G. Li, B. Gao, Q. Yue, X. Li, Characterization and ciprofloxacin adsorption properties of activated carbons prepared from biomass wastes by H_3PO_4 activation, Bioresour. Technol., 217 (2016) 239–244.
[31] Y. Huang, E. Ma, G. Zhao, Thermal and structure analysis on reaction mechanisms during the preparation of activated carbon fibers by KOH activation from liquefied wood-based fibers, Ind. Crops Prod., 69 (2015) 447–455.
[32] Y. Zhuang, Q.Z. Liu, Y. Kong, C.C. Shen, H.T. Hao, D.D. Dionysiou, B.Y. Shi, Enhanced antibiotic removal through a dual-reaction-center Fenton-like process in 3D graphene based hydrogels, Environ. Sci.-Nano, 6 (2019) 388–398.
[33] Y. Zhuang, F. Yu, J. Ma, J.H. Chen, Enhanced adsorption removal of antibiotics from aqueous solutions by modified alginate/graphene double network porous hydrogel, J. Colloid. Interface Sci., 507 (2017) 250–259.
[34] H. Liu, Y.F. Wei, J.M. Luo, T. Li, D. Wang, S.L. Luo, J.C. Crittenden, 3D hierarchical porous-structured biochar aerogel for rapid and efficient phenicol antibiotics removal from water, Chem. Eng. J., 368 (2019) 639–648.
[35] P. Ndagijimana, X.J. Liu, G.W. Yu, Y. Wang, Synthesis of a novel core-shell-structure activated carbon material and its application in sulfamethoxazole adsorption, J. Hazard. Mater., 368 (2019) 602–612.
[36] Y. Chao, W. Zhu, B. Yan, Y. Lin, S. Xun, H. Ji, X. Wu, H. Li, Changri, Macroporous polystyrene resins as adsorbents for the removal of tetracycline antibiotics from an aquatic environment, J. Appl. Polym. Sci., 131 (2014) 40561.
[37] P. Liu, W.J. Liu, H. Jiang, J.J. Chen, W.W. Li, H.Q. Yu, Modification of bio-char derived from fast pyrolysis of biomass and its application in removal of tetracycline from aqueous solution, Bioresour. Technol., 121 (2012) 235–240.
[38] L. Huang, M. Wang, C. Shi, J. Huang, B. Zhang, Adsorption of tetracycline and ciprofloxacin on activated carbon prepared from lignin with H_3PO_4 activation, Desal. Wat. Treat., 52 (2014) 2678–2687.
[39] G.Z. Liu, Z.L. Zhu, Y.X. Yang, Y.R. Sun, F. Yu, J. Ma, Sorption behavior and mechanism of hydrophilic organic chemicals to virgin and aged microplastics in freshwater and seawater, Environ. Pollut., 246 (2019) 26–33.
[40] S. Chen, J. Hong, H. Yang, J. Yang, Adsorption of uranium (VI) from aqueous solution using a novel graphene oxide-activated carbon felt composite, J. Environ. Radioact., 126 (2013) 253–258.